13

CR Formulation Overview II

TABLE OF CONTENTS

This Chapter contuinues the overview of the CR fomulation that began in the previous Chapter. Appendix material and References have been placed in Appendix R.

§13.1. Internal Forces

The element internal force vector $\bar{\mathbf{p}}^e$ and tangent stiffness matrix $\bar{\mathbf{K}}^e$ are computed in the CR configuration based on small deformational displacements and rotations. Variations of the element DOF, collected in $\mathbf{v}_d^e$ as indicated in Table 13.2, must be linked to variations in the global frame to flesh out the EICR interface of Figure 12.4. This section develops the necessary relations.

§13.1.1. Force Transformations

Consider an individual element e with N^e nodes with six DOF (three translations and three rotations) at each. Assume the element to be linearly elastic, undergoing only small deformations. Its internal energy is assumed to be a function of the deformational displacements: $U^e = U^e(\bar{\mathbf{v}}_d^e)$, with array $\bar{\mathbf{v}}_d^e$ organized as shown in Table 13.2. U^e is a frame independent scalar. The element internal force vector $\bar{\mathbf{p}}^e$ in the CR frame is given by $\bar{\mathbf{p}}^e = \partial U^e/\partial \bar{\mathbf{v}}_d^e$. For each node $a = 1, \ldots N^e$:

$$\bar{\mathbf{p}}_a^e = \frac{\partial U^e}{\partial \bar{\mathbf{v}}_{da}^e}, \quad \text{or} \quad \begin{bmatrix} \bar{\mathbf{p}}_{ua}^e \\ \bar{\mathbf{p}}_{\theta a}^e \end{bmatrix} = \begin{bmatrix} \dfrac{\partial U^e}{\partial \bar{\mathbf{u}}_{da}} \\ \dfrac{\partial U^e}{\partial \bar{\boldsymbol{\theta}}_{da}} \end{bmatrix} \tag{13.1}$$

where the second form separates the translational and rotational (moment) forces. To refer these to the global frame we need to relate local-to-global kinematic variations:

$$\begin{bmatrix} \delta\bar{\mathbf{u}}_{da}^e \\ \delta\bar{\boldsymbol{\theta}}_{da}^e \end{bmatrix} = \sum_{b=1}^{N^e} \mathbf{J}_{ab} \begin{bmatrix} \delta\mathbf{u}_a^e \\ \delta\boldsymbol{\omega}_a^e \end{bmatrix}, \quad \mathbf{J}_{ab} = \begin{bmatrix} \dfrac{\partial\bar{\mathbf{u}}_{db}^e}{\partial\mathbf{u}_a^e} & \dfrac{\partial\bar{\mathbf{u}}_{db}^e}{\partial\boldsymbol{\omega}_a^e} \\ \dfrac{\partial\bar{\boldsymbol{\theta}}_{db}^e}{\partial\mathbf{u}_a^e} & \dfrac{\partial\bar{\boldsymbol{\theta}}_{db}^e}{\partial\boldsymbol{\omega}_a^e} \end{bmatrix}. \tag{13.2}$$

From virtual work invariance, $(\bar{\mathbf{p}}_u^e)^T\delta\bar{\mathbf{u}}_d^e + (\bar{\mathbf{p}}_\theta^e)^T\delta\bar{\boldsymbol{\theta}}_d^e = (\mathbf{p}_u^e)^T\delta\mathbf{u}^e + (\mathbf{p}_\theta^e)^T\delta\boldsymbol{\omega}^e$, whence

$$\begin{bmatrix} \mathbf{p}_{ua}^e \\ \mathbf{p}_{\theta a}^e \end{bmatrix} = \sum_{b=1}^{N^e} \mathbf{J}_{ab}^T \begin{bmatrix} \bar{\mathbf{p}}_{ua}^e \\ \bar{\mathbf{p}}_{\theta a}^e \end{bmatrix}, \quad a = 1, \ldots N^e. \tag{13.3}$$

It is convenient to split the Jacobian in (13.2) as $\mathbf{J}_{ab} = \bar{\mathbf{H}}_b\bar{\mathbf{P}}_{ab}\mathbf{T}_a$ and $\mathbf{J}_{ab}^T = \mathbf{T}_a^T\bar{\mathbf{P}}_{ab}^T\bar{\mathbf{H}}_b^T$. These matrices are provided from three transformation stages, flowcharted in Figure 13.1:

$$\begin{aligned}
&\begin{bmatrix} \delta\bar{\mathbf{u}}_{db}^e \\ \delta\bar{\boldsymbol{\theta}}_{db}^e \end{bmatrix} = \begin{bmatrix} \mathbf{I} & \mathbf{0} \\ \mathbf{0} & \bar{\mathbf{H}}_{db} \end{bmatrix} \begin{bmatrix} \delta\bar{\mathbf{u}}_b^e \\ \delta\bar{\boldsymbol{\omega}}_b^e \end{bmatrix}, \quad \text{with } \bar{\mathbf{H}}_{db} = \begin{bmatrix} \dfrac{\partial\bar{\boldsymbol{\theta}}_{db}^e}{\partial\bar{\boldsymbol{\omega}}_{db}^e} \end{bmatrix}, \\
&\begin{bmatrix} \delta\bar{\mathbf{u}}_b^e \\ \delta\bar{\boldsymbol{\omega}}_b^e \end{bmatrix} = \bar{\mathbf{P}}_{ab} \begin{bmatrix} \delta\bar{\mathbf{u}}_a^e \\ \delta\bar{\boldsymbol{\omega}}_a^e \end{bmatrix}, \quad \text{with } \bar{\mathbf{P}}_{ab} = \begin{bmatrix} \dfrac{\partial\bar{\mathbf{u}}_{db}^e}{\partial\bar{\mathbf{u}}_a^e} & \dfrac{\partial\bar{\mathbf{u}}_{db}^e}{\partial\bar{\boldsymbol{\omega}}_a^e} \\ \dfrac{\partial\bar{\boldsymbol{\omega}}_{db}^e}{\partial\bar{\mathbf{u}}_a^e} & \dfrac{\partial\bar{\boldsymbol{\omega}}_{db}^e}{\partial\bar{\boldsymbol{\omega}}_a^e} \end{bmatrix}, \\
&\begin{bmatrix} \delta\bar{\mathbf{u}}_a^e \\ \delta\bar{\boldsymbol{\omega}}_a^e \end{bmatrix} = \mathbf{T}_a \begin{bmatrix} \delta\mathbf{u}_a^e \\ \delta\boldsymbol{\omega}_a^e \end{bmatrix} = \begin{bmatrix} \mathbf{T}_R & \mathbf{0} \\ \mathbf{0} & \mathbf{T}_R \end{bmatrix} \begin{bmatrix} \delta\mathbf{u}_a^e \\ \delta\boldsymbol{\omega}_a^e \end{bmatrix},
\end{aligned} \tag{13.4}$$

The 3×3 matrix $\mathbf{L}$ is the Jacobian derivative already encountered in (12.19). An explicit expression in terms of $\boldsymbol{\theta}$ is given in (R.48) of Appendix A. To express compactly the transformations for the entire

element it is convenient to assemble the $6N^e \times 6N^e$ matrices

$$\bar{\mathbf{P}} = \begin{bmatrix} \bar{\mathbf{P}}_{11} & \bar{\mathbf{P}}_{12} & \ldots & \bar{\mathbf{P}}_{1N^e} \\ \bar{\mathbf{P}}_{21} & \bar{\mathbf{P}}_{22} & \ldots & \bar{\mathbf{P}}_{2N^e} \\ \ldots & \ldots & \ldots & \ldots \\ \bar{\mathbf{P}}_{N^e1} & \bar{\mathbf{P}}_{N^e2} & \ldots & \bar{\mathbf{P}}_{N^eN^e} \end{bmatrix}, \quad \mathbf{T} = \mathbf{diag}\,[\,\mathbf{T}_R \;\; \mathbf{T}_R \;\; \ldots \;\; \mathbf{T}_R\,]. \tag{13.5}$$

and $\bar{\mathbf{H}}$ is defined in (12.20).

Then the element transformations can be written

$$\delta\mathbf{v}^e_d = \bar{\mathbf{H}}\,\bar{\mathbf{P}}\,\mathbf{T}\,\delta\mathbf{v}^e, \quad \mathbf{p}^e = \mathbf{T}^T\,\bar{\mathbf{P}}^T\,\bar{\mathbf{H}}^T\,\bar{\mathbf{p}}^e. \tag{13.6}$$

The 6×6 matrix $\bar{\mathbf{P}}_{ab}$ in (13.4) extracts the deformational part of the displacement at node b in terms of the total displacement at node a, both referred to the CR frame. At the element level, $\delta\bar{\mathbf{v}}^e_d = \bar{\mathbf{P}}\,\delta\bar{\mathbf{v}}^e$ extracts the deformational part by "projecting out" the rigid body modes. For this reason $\bar{\mathbf{P}}$ is called a *projector*.

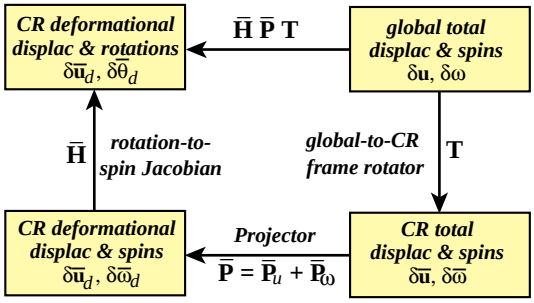

FIGURE 13.1. Staged transformation sequence from deformed to global DOFs.

As noted in Section 3.5, $\bar{\mathbf{P}}$ may be decomposed into a translational projector or T-projector $\bar{\mathbf{P}}_u$ and a rotational projector or R-projector $\bar{\mathbf{P}}_\omega$, so that $\bar{\mathbf{P}} = \bar{\mathbf{P}}_u + \bar{\mathbf{P}}_\omega$. Each has a rank of 3. The T-projector is a purely numeric matrix exemplified by (12.11). The R-projector can be expressed as $\bar{\mathbf{P}}_\omega = \bar{\mathbf{S}}\bar{\mathbf{G}}$, where $\bar{\mathbf{S}}$ is defined in (12.12) and $\bar{\mathbf{G}}$ in (12.15). Additional properties are studied below.

Remark 3. Rankin and coworkers [R.54,R.63–R.67] use an internal force transformation in which the incremental nodal rotations are used instead of the spins. This results in an extra matrix, $\bar{\mathbf{H}}^{-1}$ appearing in the sequence (13.6). The projector derived in those papers differs from the one constructed here in two ways: (1) only the R-projector is considered, and (2) the origin of the CR frame is not placed at the element centroid but at an element node defined by local node numbering. Omitting the T-projection is inconsequential if the element is "clean" with respect to translational rigid body motions [R.30, Sec. 5].

§13.1.2. Projector Properties

In this section the bar over $\mathbf{P}$, etc is omitted for brevity, since the properties described below are frame independent. In Section 3.5 it was stated without proof that (12.18) verifies the orthogonal projector property $\mathbf{P}^2 = \mathbf{P}$. Since $\mathbf{P}^2 = (\mathbf{P}_u - \mathbf{P}_\omega)^2 = \mathbf{P}_u^2 - 2\mathbf{P}_u\mathbf{P}_\omega + \mathbf{P}_\omega^2$, satisfaction requires $\mathbf{P}_u^2 = \mathbf{P}_u$, $\mathbf{P}_\omega^2 = \mathbf{P}_\omega$, and $\mathbf{P}_u\mathbf{P}_\omega = \mathbf{0}$. Verification of $\mathbf{P}_u^2 = \mathbf{P}_u$ is trivial. Recalling that $\mathbf{P}_\omega = \mathbf{SG}$ we get

$$\mathbf{P}_\omega^2 = \mathbf{S}\,(\mathbf{G}\,\mathbf{S})\,\mathbf{G} = \mathbf{S}\,\mathbf{I}\,\mathbf{G} = \mathbf{S}\,\mathbf{G} = \mathbf{P}_\omega. \tag{13.7}$$

This assumes $\mathbf{D} = \mathbf{I}$ in (12.17); verification for non-identity $\mathbf{D}$ is immediate upon removal of zero rows and columns. The orthogonality property $\mathbf{P}_u\,\mathbf{P}_\omega = \mathbf{P}_u\,\mathbf{S}\,\mathbf{G} = \mathbf{0}$ follows by observing that $\mathbf{Spin}(\mathbf{x}_C) = \mathbf{0}$, where $\mathbf{x}_C$ are the coordinates of the element centroid in any frame with origin at C.

In the derivation of the consistent tangent stiffness, the variation of $\mathbf{P}^T$ contracted with a force vector $\mathbf{f}$, where $\mathbf{f}$ is not varied, is required. The variation of the projector can be expressed as

$$\delta\mathbf{P} = \delta\mathbf{P}_u - \delta\mathbf{P}_\omega = -\delta\mathbf{P}_\omega = -\delta\mathbf{S}\,\mathbf{G} - \mathbf{S}\,\delta\mathbf{G}. \tag{13.8}$$

For the tangent stiffness one needs $\delta\mathbf{P}^T\,\mathbf{f}$. This vector can be decomposed into a balanced (self-equilibrated) force $\mathbf{f}_b = \mathbf{Pf}$ and an unbalanced (out of equilibrium) force $\mathbf{f}_u = (\mathbf{I} - \mathbf{P})\mathbf{f}$. Then

$$\begin{aligned} \delta\mathbf{P}^T\,\mathbf{f} &= -(\mathbf{G}^T\,\delta\mathbf{S}^T + \delta\mathbf{G}^T\,\mathbf{S}^T)\,(\mathbf{f}_b + \mathbf{f}_u) = -\mathbf{G}^T\,\delta\mathbf{S}^T\,\mathbf{P}^T\,\mathbf{f} - (\mathbf{G}^T\,\delta\mathbf{S}^T + \delta\mathbf{G}^T\,\mathbf{S}^T)\,\mathbf{f}_u \\ &= -\mathbf{G}^T\,\delta\mathbf{S}^T\,\mathbf{P}^T\,\mathbf{f} + \delta\mathbf{P}^T\,\mathbf{f}_u. \end{aligned} \tag{13.9}$$

where $\mathbf{S}^T\,\mathbf{f}_b = \mathbf{0}$ was used. This comes from the fact that the columns of $\mathbf{S}$ are the three rotational rigid body motions, which do not produce work on an self-equilibrated force vector.

The term $\delta\mathbf{P}^T\,\mathbf{f}_u$ will be small if element configurations $\mathcal{C}^R$ and $\mathcal{C}^D$ are close because in this case $\mathbf{f}_u$ will approach zero. If $\mathbf{G}$ has the factorizable form shown below, however, we can show that $\delta\mathbf{P}^T\,\mathbf{f}_u = \mathbf{0}$ identically, regardless of how close $\mathcal{C}^R$ and $\mathcal{C}^D$ are, as long as $\mathbf{f}$ is in translational equilibrium. Assume that $\mathbf{G}$ can be factored as

$$\mathbf{G} = \mathbf{\Xi}\,\mathbf{\Gamma}, \quad \text{with} \quad \delta\mathbf{G} = \delta\mathbf{\Xi}\,\mathbf{\Gamma}. \tag{13.10}$$

where $\mathbf{\Xi}$ is a coordinate dependent invertible 3×3 matrix, and $\mathbf{\Gamma}$ is a constant $3\times 6N^e$ matrix. Since $\mathbf{G}\mathbf{S} = \mathbf{I}$ as per (12.17), $\mathbf{\Xi}^{-1} = \mathbf{\Gamma}\,\mathbf{S}$, and $\delta\mathbf{G}\,\mathbf{S} + \mathbf{G}\,\delta\mathbf{S} = \delta\mathbf{\Xi}\,\mathbf{\Gamma}\,\mathbf{S} + \mathbf{G}\,\delta\mathbf{S} = 0$, whence $\delta\mathbf{\Xi} = -\mathbf{G}\,\delta\mathbf{S}\,\mathbf{\Xi}$. Then

$$\begin{aligned}
\delta\mathbf{P}^T\,\mathbf{f}_u &= -(\mathbf{G}^T\,\delta\mathbf{S}^T + \mathbf{\Gamma}^T\,\delta\mathbf{\Xi}^T\,\mathbf{S}^T)\,\mathbf{f}_u = -(\mathbf{G}^T\,\delta\mathbf{S}^T - \mathbf{\Gamma}^T\,\mathbf{\Xi}^T\,\delta\mathbf{S}^T, \mathbf{G}^T\,\mathbf{S}^T)\,\mathbf{f}_u \\
&= -(\mathbf{G}^T\,\delta\mathbf{S}^T - \mathbf{G}^T\,\delta\mathbf{S}^T\,\mathbf{P}_\omega^T)\,\mathbf{f}_u = -(\mathbf{G}^T\,\delta\mathbf{S}^T(\mathbf{I} - \mathbf{P}_\omega^T)\,\mathbf{f}_u = -\mathbf{G}^T\,\delta\mathbf{S}^T(\mathbf{I} - \mathbf{P}_\omega^T)\,\mathbf{f}_u \\
&= -\mathbf{G}^T\,\delta\mathbf{S}^T(\mathbf{I} - \mathbf{P}_\omega^T)(\mathbf{I} - \mathbf{P}^T)\,\mathbf{f} = \mathbf{0},
\end{aligned} \tag{13.11}$$

if $\mathbf{f}$ is in translational equilibrium: $\mathbf{f} = \mathbf{P}_\omega^T\,\mathbf{f}$. This is always satisfied for any element that represents rigid body translations correctly [R.30, Sec. 5].

§13.2. Tangent Stiffness

We consider here only the stiffness derived from the internal energy. The load stiffness due to nonconservative forces, such as aerodynamic pressures, has to be treated separately.

§13.2.1. Definition

The consistent tangent stiffness matrix $\mathbf{K}^e$ of element e is defined as the variation of the internal forces with respect to element global freedoms:

$$\delta\mathbf{p}^e \stackrel{\text{def}}{=} \mathbf{K}^e\,\delta\mathbf{v}^e, \quad \text{whence} \quad \mathbf{K}^e = \frac{\partial\mathbf{p}^e}{\partial\mathbf{v}^e}. \tag{13.12}$$

Taking the variation of $\mathbf{p}^e$ in (13.6) gives rise to four terms:

$$\begin{aligned}
\delta\mathbf{p}^e &= \delta\mathbf{T}^T\,\bar{\mathbf{P}}^T\,\bar{\mathbf{H}}^T\,\bar{\mathbf{p}}^e + \mathbf{T}^T\,\delta\bar{\mathbf{P}}^T\,\bar{\mathbf{H}}^T\,\bar{\mathbf{p}}^e + \mathbf{T}^T\,\bar{\mathbf{P}}^T\,\delta\mathbf{H}^T\,\bar{\mathbf{p}}^e + \mathbf{T}^T\,\bar{\mathbf{P}}^T\,\bar{\mathbf{H}}^T\,\delta\bar{\mathbf{p}}^e \\
&= (\mathbf{K}^e_{GR} + \mathbf{K}^e_{GP} + \mathbf{K}^e_{GM} + \mathbf{K}^e_M)\,\delta\mathbf{v}^e.
\end{aligned} \tag{13.13}$$

The four terms identified in (13.13) receive the following names. $\mathbf{K}_M$ is the *material stiffness*, $\mathbf{K}_{GM}$ the *moment-correction geometric stiffness*, $\mathbf{K}_{GP}$ the *equilibrium projection geometric stiffness*, and $\mathbf{K}_{GR}$ the *rotational geometric stiffness*. If nodal eccentricities treated by rigid links are considered, one more term appears, called the *eccentricity geometric stiffness*. This term is studied in great detail in [R.37].

§13.2.2. Material Stiffness

The material stiffness is generated by the variation of the element internal forces $\mathbf{p}^e$:

$$\mathbf{K}^e_M\,\delta\mathbf{v}^e = \mathbf{T}_R^T\,\bar{\mathbf{P}}^T\,\bar{\mathbf{H}}^T\,\delta\bar{\mathbf{p}}^e. \tag{13.14}$$

The linear stiffness matrix in terms of the deformational freedoms in $\bar{\mathbf{v}}^e_d$ is defined as the Hessian of the internal energy:

$$\bar{\mathbf{K}}^e = \frac{\partial^2\bar{U}^e}{\partial\bar{\mathbf{v}}^e_d\partial\bar{\mathbf{v}}^e_d} = \frac{\partial\bar{\mathbf{p}}^e}{\partial\bar{\mathbf{v}}^e_d} \tag{13.15}$$

Using the transformation of $\delta\bar{\mathbf{v}}^e$ in (13.6) gives

$$\mathbf{K}^e_M = \mathbf{T}^T\,\bar{\mathbf{P}}^T\,\bar{\mathbf{H}}^T\,\bar{\mathbf{K}}^e\,\bar{\mathbf{H}}\,\bar{\mathbf{P}}\,\mathbf{T}. \tag{13.16}$$

Thus the material stiffness is given by a congruential transformation of the local stiffness $\bar{\mathbf{K}}^e$ to the global frame. This is formally the same as in linear analysis but here the transformation terms depend on the state. The expression (13.16) is valid only if $\mathbf{K}^e$ is independent of the deformational $\bar{\mathbf{v}}^e_d$ freedoms.

§13.2.3. Geometric Stiffness

To express compactly the geometric stiffness components it is convenient to introduce the arrays

$$\bar{\mathbf{p}}^e_P = \bar{\mathbf{P}}^T\,\bar{\mathbf{H}}^T\,\bar{\mathbf{p}}^e = \begin{bmatrix} \bar{\mathbf{n}}^e_1 \\ \bar{\mathbf{m}}^e_1 \\ \vdots \\ \bar{\mathbf{n}}^e_{N^e} \\ \bar{\mathbf{m}}^e_{N^e} \end{bmatrix}, \quad \bar{\mathbf{F}}_n = \begin{bmatrix} \mathbf{Spin}(\bar{\mathbf{n}}^e_1) \\ \mathbf{0} \\ \vdots \\ \mathbf{Spin}(\bar{\mathbf{n}}^e_{N^e}) \\ \mathbf{0} \end{bmatrix}, \quad \bar{\mathbf{F}}_{mn} = \begin{bmatrix} \mathbf{Spin}(\bar{\mathbf{n}}^e_1) \\ \mathbf{Spin}(\bar{\mathbf{m}}^e_1) \\ \vdots \\ \mathbf{Spin}(\bar{\mathbf{n}}^e_{N^e}) \\ \mathbf{Spin}(\bar{\mathbf{m}}^e_{N^e}) \end{bmatrix}. \tag{13.17}$$

These are filled with the *projection node forces* $\bar{\mathbf{p}}^e_P$. Only the final form of the geometric stiffness components is given below, omitting the detail derivations of [R.37]. The rotational geometric stiffness is generated by the variation of $\mathbf{T}$: $\mathbf{K}^e_{RG}\,\delta\mathbf{v}^e = \delta\mathbf{T}^T\,\bar{\mathbf{P}}^T\,\bar{\mathbf{H}}^T\,\bar{\mathbf{p}}^e$ and can be expressed as

$$\mathbf{K}_{GR} = -\mathbf{T}^T\,\bar{\mathbf{F}}_{nm}\,\bar{\mathbf{G}}\,\mathbf{T}, \tag{13.18}$$

$\mathbf{K}^e_{RG}$ is the gradient of the internal force vector with respect to the rigid rotation of the element. This interpretation is physically intuitive because a rigid rotation of a stressed element necessarily reorients the stress vectors by that amount. Consequently the internal element forces must rigidly rotate to preserve equilibrium.

The moment-correction geometric stiffness is generated by the variation of the jacobian $\mathbf{H}$: $\mathbf{K}^e_{RG}\delta\mathbf{v}^e = \mathbf{T}^T_R\,\bar{\mathbf{P}}^T\,\delta\bar{\mathbf{H}}^T\,\bar{\mathbf{p}}^e$. It is given by

$$\mathbf{K}^e_{GM} = \mathbf{T}^T\,\bar{\mathbf{P}}^T\bar{\mathbf{L}}\,\bar{\mathbf{P}}\mathbf{T}. \tag{13.19}$$

where $\mathbf{L}$ is defined in Section 3.5.

The equilibrium projection geometric stiffness arises from the variation of the projector $\bar{\mathbf{P}}$ with respect to the deformed element geometry: $\mathbf{K}^e_{GP}\delta\mathbf{v}^e = \mathbf{T}^T_R\,\delta\mathbf{P}^T\,\mathbf{H}^T\,\bar{\mathbf{p}}^e$. As in Section 4.2, decompose $\bar{\mathbf{p}}^e$ into a balanced (self-equilibrated) force $\bar{\mathbf{p}}^e_b = \bar{\mathbf{P}}^T\,\bar{\mathbf{p}}^e$ and an unbalanced force $\bar{\mathbf{p}}^e_u = \bar{\mathbf{p}}^e - \bar{\mathbf{p}}^e_b$. If $\delta\bar{\mathbf{P}}^T\,\bar{\mathbf{p}}^e_u$ is either identically zero or may be neglected as discussed in Section 4.2, $\mathbf{K}^e_{GP}$ is given by

$$\mathbf{K}_{GP} = -\mathbf{T}^T\,\bar{\mathbf{G}}^T\,\bar{\mathbf{F}}_n\,\bar{\mathbf{P}}\,\mathbf{T}, \tag{13.20}$$

in which the balanced force $\bar{\mathbf{p}}^e_b$ is used in (13.17) to get $\bar{\mathbf{F}}_n$.

If $\mathbf{T}^T\,\delta\bar{\mathbf{P}}^T\,\bar{\mathbf{p}}^e_u$ cannot be neglected, as may happen in highly warped shell elements in a coarse mesh, the following correction term may be added to $\mathbf{K}^e_{RG}$:

$$\Delta\mathbf{K}_{GP} = -\mathbf{T}^T\left(\bar{\mathbf{G}}^T\,\bar{\mathbf{F}}_{nu}\,\bar{\mathbf{P}} + \frac{\partial\mathbf{G}}{\partial\mathbf{v}}\,\bar{\mathbf{S}}\,\bar{\mathbf{p}}^e_u\right)\mathbf{T}, \tag{13.21}$$

where $\mathbf{F}_{nu}$ is $\mathbf{F}_n$ of (13.17) when $\bar{\mathbf{p}}^e_u$ is inserted instead of $\bar{\mathbf{p}}^e$. In the computations reported in Part II [R.38] this term was not included.

$\mathbf{K}^e_{RG}$ expresses the variation of the projection of the internal force vector $\bar{\mathbf{p}}_e$ as the element geometry changes. This can be interpreted mathematically as follows: In the vector space of element force vectors the subspace of self-equilibrium force vectors changes as the element geometry changes. The projected force vector thus has a gradient with respect to the changing self-equilibrium subspace, even though the element force $\bar{\mathbf{f}}_e$ does not change.

The complete form of the element tangent stiffness, excluding correction terms (13.21) for highly warped elements, is

$$\mathbf{K}^e = \mathbf{T}^T\big(\bar{\mathbf{P}}^T\bar{\mathbf{H}}^T\,\bar{\mathbf{K}}^e\,\bar{\mathbf{H}}\,\bar{\mathbf{P}} + \bar{\mathbf{P}}^T\,\bar{\mathbf{L}}\,\bar{\mathbf{P}} - \bar{\mathbf{F}}_{nm}\,\bar{\mathbf{G}} - \bar{\mathbf{G}}^T\,\bar{\mathbf{F}}_n^T\,\bar{\mathbf{P}}\big)\mathbf{T} = \mathbf{T}^T\,\bar{\mathbf{K}}^e_P\mathbf{T}, \tag{13.22}$$

in which $\bar{\mathbf{K}}^e_R$, which is the *local tangent stiffness matrix* (the tangent stiffness matrix in the local CR frame of the element) is given by the parenthesized expression.

§13.2.4. Consistency Verification

The local tangent stiffness matrix $\bar{\mathbf{K}}^e_R$ given in (13.22) has some properties that may be exploited to verify the computer implementation [R.54,R.37]:

$$\begin{aligned}&\bar{\mathbf{K}}^e_R\,\bar{\mathbf{S}} = -\bar{\mathbf{F}}_{nm}, \quad \bar{\mathbf{S}}^T\,\bar{\mathbf{K}}^e_R = -\mathbf{F}_n^T, \quad \bar{\mathbf{K}}_M\,\bar{\mathbf{S}} = \mathbf{0}, \quad \bar{\mathbf{K}}_{GR}\,\bar{\mathbf{S}} = -\bar{\mathbf{F}}_{nm},\\ &\bar{\mathbf{K}}_{GP}\,\bar{\mathbf{S}} = \mathbf{0}, \quad \bar{\mathbf{S}}^T\,\bar{\mathbf{K}}_M = \mathbf{0}, \quad \bar{\mathbf{S}}^T\,(\bar{\mathbf{K}}_{GR} + \bar{\mathbf{K}}_{GP}) = -\bar{\mathbf{F}}_n^T.\end{aligned} \tag{13.23}$$

In addition, rigid-body-mode tests on the linear stiffness matrix $\bar{\mathbf{K}}^e$ using linearized projectors are discussed in [R.30]. The set (13.23) tests the programming of the nonlinear projector $\bar{\mathbf{P}}$ since it checks the null space of $\mathbf{P}$. It also indicates whether the projector matrix is used correctly in the stiffness formulation. However, satisfaction does not fully guarantee consistency between the internal force and the tangent stiffness because $\bar{\mathbf{H}}$ and $\bar{\mathbf{L}}$ are left unchecked. Full verification of consistency can be numerically done through finite difference techniques.

§13.3. Three Consistent CR Formulations

From the foregoing unified forms of the internal force and tangent stiffness, three CR consistent formulations can be obtained by making simplifying assumptions at the internal force level. These satisfy self-equilibrium and symmetry to varying degree. The following subsections describe the three versions in order of increasing complexity. For all formulations one can take in account DOFs at eccentric nodes as described in [R.37].

§13.3.1. Consistent CR formulation (C)

This variant is that developed by Bergan and coworkers in the 1980s at Trondheim and summarized in the review article [R.56]. The internal force (13.6) is simplified by taking $\bar{\mathbf{H}} = \mathbf{I}$ and $\bar{\mathbf{P}} = \mathbf{I}$, while retaining $\delta\bar{\mathbf{v}}^e_d = \bar{\mathbf{H}}\bar{\mathbf{P}}\,\delta\bar{\mathbf{v}}^e$ for recovery of deformational DOFs. Since $\delta\bar{\mathbf{P}} = \delta\bar{\mathbf{H}} = \mathbf{0}$, the expression for the tangent stiffness of (13.13) simplifies to the material and rotational geometric stiffness terms:

$$\mathbf{p}^e = \mathbf{T}^T\,\bar{\mathbf{K}}^e\,\bar{\mathbf{v}}^e_d, \qquad \mathbf{K}^e = \mathbf{T}^T(\bar{\mathbf{K}}^e\,\bar{\mathbf{H}}\,\bar{\mathbf{P}} - \bar{\mathbf{F}}_{nm}\,\bar{\mathbf{G}})\mathbf{T}. \tag{13.24}$$

Here $\bar{\mathbf{F}}_{nm}$ is computed according to (13.17) with $\bar{\mathbf{p}}^e = \bar{\mathbf{K}}^e\bar{\mathbf{v}}_d$. The internal force is in equilibrium with respect to the CR configuration $\mathcal{C}^R$. For a shell structure, the material stiffness approaches symmetry as the element mesh is refined if the membrane strains are small. As the mesh is refined, the deformational rotation axial vectors $\bar{\boldsymbol{\theta}}_{da}$ become smaller and approach vector properties that in turn make $\mathbf{H}(\boldsymbol{\theta}_{da}$

approach the identity matrix. With small membrane strains $\bar{\mathbf{K}}^e$ is indifferent with respect to post-multiplication with $\bar{\mathbf{P}}$ because the $\mathcal{C}^R$ and $\mathcal{C}$ configurations will be close and $\bar{\mathbf{K}}^e\bar{\mathbf{P}} \to \bar{\mathbf{K}}^e$. The consistent geometric stiffness is always unsymmetric, even at equilibrium. Because of this fact one cannot expect quadratic convergence for this formulation if a symmetric solver is used.

This formulation may be unsatisfactory for warped quadrilateral shell elements since the $\mathcal{C}^R$ and $\mathcal{C}^D$ reference configurations may be far apart. Only in the limit of a highly refined element mesh will the $\mathcal{C}^R$ and $\mathcal{C}^D$ references in general be close, and satisfactory equilibrium ensured.

§13.3.2. Consistent Equilibrated CR Formulation (CE)

The internal force (13.6) is simplified by taking $\bar{\mathbf{H}} = \mathbf{I}$ so $\delta\mathbf{H} = \mathbf{0}$, but the projector $\bar{\mathbf{P}}$ is retained. This gives

$$\mathbf{p}^e = \mathbf{T}^T\bar{\mathbf{P}}^T\,\bar{\mathbf{K}}^e\,\bar{\mathbf{v}}^e_d, \qquad \mathbf{K}^e = \mathbf{T}^T(\bar{\mathbf{P}}^T\,\bar{\mathbf{K}}^e\,\bar{\mathbf{H}}\,\bar{\mathbf{P}} - \bar{\mathbf{F}}_{mn}\,\bar{\mathbf{G}} - \bar{\mathbf{G}}^T\,\bar{\mathbf{F}}_n^T\,\bar{\mathbf{P}})\mathbf{T}. \tag{13.25}$$

where $\bar{\mathbf{F}}_{nm}$ and $\bar{\mathbf{F}}_n$ are computed according to (13.17) with $\bar{\mathbf{p}}^e = \bar{\mathbf{P}}^T\bar{\mathbf{K}}^e\bar{\mathbf{v}}^e_d$.

Due to the presence of $\bar{\mathbf{P}}$ on both sides, the material stiffness of the CE formulation approaches symmetry as the mesh is refined regardless of strain magnitude. The geometric stiffness at the element level is non-symmetric, but the assembled global geometric stiffness will become symmetric as global equilibrium is approached, provided that there are no applied nodal moments and that displacement boundary conditions are conserving. A symmetrized global tangent stiffness maintains quadratic convergence for refined element meshes with this formulation.

§13.3.3. Consistent Symmetrizable Equilibrated CR Formulation (CSE)

All terms in (13.6) are retained, giving

$$\mathbf{p}^e = \mathbf{T}^T\bar{\mathbf{P}}^T\,\bar{\mathbf{H}}^T\,\bar{\mathbf{K}}^e\,\bar{\mathbf{v}}^e_d, \quad \mathbf{K}^e = \mathbf{T}^T(\bar{\mathbf{P}}^T\,\bar{\mathbf{H}}^T\,\bar{\mathbf{K}}^e\bar{\mathbf{H}}\,\bar{\mathbf{P}} + \bar{\mathbf{P}}^T\,\bar{\mathbf{L}}\,\bar{\mathbf{P}} - \bar{\mathbf{F}}_{nm}\,\bar{\mathbf{G}} - \bar{\mathbf{G}}^T\,\bar{\mathbf{F}}_n^T\,\bar{\mathbf{P}})\mathbf{T}. \tag{13.26}$$

where $\bar{\mathbf{F}}_{nm}$ and $\bar{\mathbf{F}}_n$ are computed according to (13.17) with $\bar{\mathbf{f}} = \bar{\mathbf{P}}^T\,\bar{\mathbf{H}}\,\bar{\mathbf{K}}^e\,\bar{\mathbf{v}}^e_d$. The assembled global geometric stiffness for this formulation becomes symmetric as global equilibrium is approached, as in the CE case, as long as there are no applied nodal moments and the loads as well as boundary conditions are conserving. Since the material stiffness is always symmetric, quadratic convergence with a symmetrized tangent stiffness can be exppected without the refined-mesh-limit assumption of the CE formulation.

Remark 4. The relative importance of including the **H** matrix, which is neglected by most authors, and the physical significance of this Jacobian term are discussed in Part II [R.38].

§13.3.4. Formulation Requirements

It is convenient to set forward a set of requirements for geometrically nonlinear analysis with respect to which different CR formulations can be evaluated. They are listed below in order of decreasing importance.

Equilibrium. By this requirement is meant: to what extent the finite element internal force vector **p** is in self-equilibrium with respect to the deformed configuration $\mathcal{C}^D$? This is a fundamental requirement for tracing the correct equilibrium path in an incremental-iterative solution procedure.

Consistency. A formulation is called consistent if the tangent stiffness is the gradient of the internal forces with respect to the global DOF. This requirement determines the convergence rate of an incremental-iterative solution algorithm. An inconsistent tangent stiffness may give poor convergence, but does not

Table 13.4. Attributes of Corotated Formulations C, CE and CSE.

Formulation	*Self-equil.*(1)	*Consistent*(2)	*Invariant*(3)	*Symmetriz.*(4)	*Elem.Indep.*(5)
C		√	√		√
CE	√	√	√		√
CSE	√	√	√	√	√

(1) checked if element is in self-equilibrium in deformed configuration $\mathcal{C}^D$.
(2) checked if tangent stiffness is the **v** gradient of the element internal force.
(3) checked if the formulation is insensitive to choice of node numbering.
(4) checked if formulation maintains quadratic convergence of a true Newton solution algorithm with a symmetrized tangent stiffness matrix.
(5) checked if the matrix and vector operations that account for geometrically nonlinear effects are the same for all elements with the same node and DOF configuration.

alter the equilibrium path since this is entirely prescribed by the foregoing equilibrium requirement. However, lack of consistency may affect the location of bifurcation (buckling) points and the branch switching mechanism for post-buckling analysis. In other words, an inconsistent tangent stiffness matrix may detect ("see") a bifurcation where equilibrium is not satisfied from the residual equation. Subsequent traversal by branch-switching will then be difficult because the corrector iterations need to jump to the secondary path as seen by the residual equation.

Invariance. This requirement refers to whether the solution is insensitive to internal choices that may depend on node numbering. For example, does a local element-node reordering give an altered equilibrium path or change the convergence characteristics for the analysis for an otherwise identical mesh? The main contributor to lack of invariance is the way the deformational displacement vector is extracted from the total displacements, if the extraction is affected by the choice of the local CR frame. If lack of invariance is observed, it may be usually traced to the matrix **G**, which links the variation of the rigid body rotation to that of the nodal DOF degrees of freedom.

Symmetrizability. This means that a symmetrized **K** can be used without loss of quadratic convergence rate in a true Newton solver even when the consistent tangent stiffness away from equilibrium is not symmetric. In the examples studied in Part II [R.38] this requirement was met when the material stiffness of the formulation was rendered symmetric.

Element Independence. This is used in the sense of the EICR discussed in Section 2.5. It means that the matrix and vector operations that account for geometrically nonlinear effects are the same for all elements that possess the same node and DOF configuration.

Attributes of the C, CE and CSE formulations in light of the foregoing requirements are summarized in Table 13.4.

§13.3.5. Limitations of the EICR Formulation

The present CR framework, whether used in the C, CE or CSE formulation variants, is element independent in the EICR sense discussed in Section 2.5 since it does not contain gradients of intrinsically element dependent quantities such as the strain-displacement relationship. This treatment is appropriate for elements where the restriction to small strains automatically implies that the CR and deformed element configurations are close. This holds automatically for low order models such as two-node straight bars and beams, and three-node facet shell elements.

The main reason for limiting element independence to low-order elements is the softening effect of the nonlinear projector **P**. The use of **P** to restore the correct rigid body motions, and hence equilibrium with

respect to the deformed element geometry, effectively reduces the eigenvalues of the material stiffness relative to the CR material stiffness $\bar{\mathbf{K}}_e$ before projection. This softening effect becomes significant if the $\mathcal{C}^R$ and $\mathcal{C}^D$ geometries are far apart.

Such softening effects are noticeable in four-node initially-warped shell elements. Assume that the element is initially warped with "positive" warping, and consider only the effect of $\mathbf{P}$. The element material stiffness of this initial positive warping is then $\mathbf{K}_+ = \mathbf{P}_+^T \mathbf{K}_e \mathbf{P}_+ = \mathbf{K}_e$. Apply displacements that switch this warping to the opposite of the initial one; that is, a "negative" warping. The new element material stiffness then becomes $\mathbf{K}_- = \mathbf{P}_-^T \mathbf{K}_e \mathbf{P}_- \neq \mathbf{K}_e$ One will intuitively want the two element configurations to have the same rigidity in the sense of the dominant nonzero eigenvalues of the tangent stiffness matrix. But it can be shown that the eigenvalues of the projected material stiffness matrix $\mathbf{K}_-$ can be significantly lower than those of the initial stiffness matrix $\mathbf{K}_+$. If the element stiffness $\mathbf{K}_e$ is referred to the flat element projection, one can restore symmetry of $\mathbf{K}_+$ and $\mathbf{K}_-$ with respect to dominant nonzero eigenvalues, but it is not possible to remove the softening effect.

This argument also carries over to higher order bar, arch and shell elements that are curved in the initial reference configuration. It follows that the EICR is *primarily useful for low-order elements of simple geometry*.

§13.4. Conclusions

Chapters 12 and 13 have presented a unified formulation for geometrically nonlinear analysis using the CR kinematic description, assuming small deformations. Although linear elastic material behavior has been assumed for brevity, extension to materially nonlinear behavior such as elastoplasticity and fracture within the confines of small deformations, is feasible as further discussed below. All terms in the internal force and tangent stiffness expressions are accounted for. It is shown how dropping selected terms in the former produces simpler CR versions used by previous investigators.

These versions have been tested on thin shell and flexible-mechanism structures, as reported in Part II [R.38]. Shells are modeled by triangle and quadrilateral elements. The linear stiffness of these elements is obtained with the ANDES (Assumed Natural DEviatoric Strains) formulation of high performance elements [R.27–R.32,R.53]. Test problems include benchmarks in buckling, nonlinear bifurcation and collapse.

Does the unified formulation close the book on CR? Hardly. Several topics either deserve further development or have been barely addressed:

(A) Relaxing the small-strain assumption to allow moderate deformations.

(B) Robust handling of extremely large rotations involving multiple revolutions.

(C) Integrating CR elements with rigid links and joint elements for flexible multibody dynamics.

(D) Using substructuring concepts for CR modeling of structural members with continuum elements.

(E) Achieving a unified form for CR dynamics, including nonconservative effects and multiphysics.

Topic (A) means the use of CR for problems where strains may locally reach moderate levels, say 1–10%, as in elastoplasticity and fracture, using appropriate strain and stress measures in the local frame. The challenge is that change of metric of the CR configuration should be accounted for, even if it means dropping the EICR property. Can CR compete against the more established TL and UL descriptions? It seems unreasonable to expect that CR can be of use in overall large strain problems such as metal forming, in which UL reigns supreme. But it may be competitive in *localized failure* problems, where most of the structure remain elastic although undergoing finite rotations.

Some data points are available: previous large-deformation work presented in [R.46,R.47,R.50,R.51,R.57]. More recently Skallerud et al. reported [R.75] that a submerged-pipeline failure shell code using the ANDES CR quadrilateral of [R.37] plus elastoplasticity [R.74] and fracture mechanics [R.21] was able to beat a well known commercial TL-based code by a factor of 600 in CPU time. This speedup is of obvious interest in influencing both design cycle and deployment planning.

Topic (B) is important in applications where a floating (free-free) structure undergoes several revolutions, as in combat airplane maneuvers, payload separation or orbital structure deployment. The technical difficulty is that expressions presented in the Appendix cannot handle finite rotations beyond $\pm 2\pi$, and thus require occasional resetting of the base configuration. While this can be handled via restarts for structures such as full airplanes, it can be more difficult when the *relative* rotation between components exceeds $\pm 2\pi$, as in separation, fragmentation or deployment problems.

Topics (C) and (D) have been addressed in the FEDEM program developed by SINTEF at Trondheim, Norway. This program combines CR shell and beam elements of [R.37], grouped into substructures, with kinematic objects typical of rigid-body dynamics: eccentric links and joints. Basic tools used in FEDEM for combining joint models with flexible continuum elements are covered in a recent book [R.73].

Finally, topic (E) is fertile ground for research. The handling of model components such as mass, damping and nonconservative effects in fluid-structure interaction and aeroelasticity is an active ongoing research topic. For example a recent paper [R.26] describes flight maneuver simulations of a complete F-16 fighter using CR elements to model the aircraft. As in statics, a key motivation for CR in dynamics is reuse of linear FEM force-stiffness libraries. Can that reuse extend to mass and damping libraries? And how do standard time integration methods perform when confronted with unsymmetric matrices? These topics have barely been addressed.